International Journal of Engineering Research and Development
e-ISSN: 2278-067X, **p**-ISSN: 2278-800X, www.ijerd.com
Volume 6, Issue 12 (May 2013), PP.103-111

Computational Fluid Dynamic Analysis of Notched Canard Arrangement in Cruise Missiles at Supersonic Flows.

B.Kaleeswaran[1], Kowtham Kumar.K[2], S.Ranjith Kumar[3]
[1]M.Tech(Computational Fluid Dynamics), Research Scholar, UPES-Dehradun.
[2]M.Tech (Energy Systems), Research Scholar, UPES-Dehradun
[3]Design Specialist, Diagonal CAD Centre-Chennai.

Abstract:- This paper tells about the CFD analysis of 2D Canard arrangement in supersonic cruise missiles. High heat dissipation rate causes the Canards to reduce its primary work of providing rotational stability to missile. This paper discusses about the criteria of choosing notched canard model against the present model. The models were designed in GAMBIT and analysed using FLUENT. Various pressure, temperature, velocity vector and XY plots were taken and studied as results. From the results it was clear that the new notched canard arrangement shows less heat dissipation rate against the existing models. This study would be helpful in designing new canard models for missiles esp. for Supersonic cases.

Keywords:- NotchedCanard, CFD, Supersonic, FLUENT.

I. INTRODUCTION

Missiles carry war heads to create havocs. But, for complete stability of the missiles canard arrangement is essential. Canards provide rotational stability to the missile. Similarly, for the missile to carry out its required task the payload present inside the head section of the missile should not disintegrate/undergo some chemical changes due to excessive heating under supersonic flow heat dissipation conditions. To avoid both the criteria notches (cavities) could be placed in the canard aft arrangements.

Canards are devices that enhance high stability to missiles under rotational condition. They also carry sensor arrangements inside its rabbit ear like arrangement. Sometimes canards are exposed to high heat dissipation when the missile flies at Supersonic flow conditions. Two models one existing and one proposed were analysed in this paper with Mach speed of 3.Bow shocks are formed during this conditions.Thus,reducing the surface heating in canard arrangement is a must to gain stability. Pressure variation of about 188hPawas found at thetrosphereic atmospheric of 12 Km, which was considered to be the cruising atmosphere of the supersonic missiles (source: Brahmos Aerospace) were analysed and pressure variations were obtained mathematically to be used as input values.

II. CANARD TYPES

1. Equilateral model.
2. Spherical front model.
3. Sweep Delta model.
4. Tapered delta model.
5. Rectangular model.
6. Split canard arrangement.

The spherical front model was used in many cruise missiles like Patriot PAC-3, Stingermissiles, Python.

III. ISA TABLE

The International Standard Atmospheric table [1].For pressure altitude calculations and calibrations knowledge of pressure, temperature, Mach number is essential. The standard atmospheric model is a hypothetical model.The air in the model considered is devoid of dust,moisture and water vapour.The air is considered to be of no dusty and no turbulence in the air. According to mean sea level datas;

1. Pressure $p_{o} = 101325$ N/m^2
2. Density $\rho_o = 1.225$ Kg/m^3
3. Reference temperature = 288.15 K
4. Speed of sound = 340.62 m/s

5. Acceleration due to gravity = 9.81 m/s^2

The layer of troposphere starts at about 11 Km or 36087 feet. The mean sea level is about 15^o K.This, all the parameters mentioned above correspondent to the mean sea level. The temperature reduces with respect to altitude decrease at every -6.5^o C /1000 m uptotropopause, after that temperature remains constant. Air is considered to be perfect gas within the troposphere. Within the troposphere the following pressure modeling calculation exists;

$P = P_O (1-0.0065h/T_O)^{5.2561}$ **(3.1)**

Above the troposphere temperature is constant and hence integrating of hydrostatic equation gives;

$\int_{po}^{p}(dp/p) = -g/R\int_{ho}^{h}(dh)/(To - 0.0065h)$ **(3.2)**

Integrating (3.2) with respect to constant temperature gives;

$P = P_{11}\, e\, (-g\,(h-h_{11})/RT_{11})$ **(3.3)**

Where, P_{11} = 226.32 hPa (pressure at the troposphere)
T_{11}= 216.65 K (temperature at the troposphere),
h_{11} = 11,000 m (height of the troposphere layer).
h = height of the motion of the projectile.
P= standard pressure.

In this paper the missile was considered to fly at **Supersonic cruise conditions of about 40,000 ft**. and standard pressure was obtained as **188hPa for cruise condition at 0 angle of attac**k from ISA table. These results were used in analysing the supersonic flows over the model.

IV. LITERATURE SURVEY

Aerospike model was studied by Mr Rajesh Yadav et.al [2].This paper tells about the hemispherical twin spike model analysis of the aerospikes. Actually this paper was useful in analysing the design consideration of the hemispherical shape effect in hypersonic speed. Aerospikes greatly reduces the wave drag to an extent. The heat transfer rate depends on the separation of the boundary layers. Heat flux value increases with distance from the spike root.Navier stokes equation of two dimensional axisymmetric form was used in this study. Pressure and temperature at the region of stagnation increases. But, in the spike body length a region of circulation occur with respect to the second spike. Thus due to region of circulation less pressure region is possible near to the region which decides the heat flux. In this model bow shock occurs. Thus region of high temperature (convective heating) and shear stress .Temperature raise is visible till region of reattachment. Thus, shorter aerospikes offers no resistances to reduce in pressure. But, longer spike model/increasing the length of the twin spike also reduces the pressure distribution, heat distribution near to the model.

Missile with grid fins analysis was done by Senthil et.al [3]**.**This paper was about the study of aerodynamic coefficients of missiles with grid fins at the rear section. This unconventional grid fins maintains lift at higher angle of attack. It produces less stall when compared to planar fins. It has got small hinge moments. Grid fins are lattice of aerodynamic surfaces within a box. They perform well in case of hypersonic, supersonic cases but not in transonic cases.

Rockets with grid fins was analysed by Sivaramakrishna et.al [4].This research journal tells about the analysis of the rocket configurations with the grid fins using PARAS codes (Source: PARAS is an inbuilt code of VSSC).Viscous turbulent studies were carried out in this study analysis. The study was analysed with PARAS code which was highly suitable for solving high viscous and shear flow problems .Grid fins usually gives small disturbances during the flows. Design of the squared inner grid is an important one in grid fins design analysis. These grid fins could also be folded. Grid fins doesn't experiences transonic bucket [5] when compared to the planar fins [6].

Missile nose cone with spherical cavity model was analysed by B. Kaleeswaran.et.al [7].This paper tells about the effect of cavity in the nose cone model of the missile. The paper discusses the comparative study of nose cavity model with the ordinary spherical nose model. Mainly aims to reduce the thermal effects in the nose region by creating a region of recirculation zones ahead of the nose region. This model was studied in the inviscid region with the bow shock formation at the front. The model was analysed in supersonic velocity region of Mach number 3.

V. DESIGN SPECIFICATIONS

In this study analysis a missile with a nose cavity and canard arrangement was considered. Two models were analysed in supersonic regimes. One with spherical canard arrangement and another with notched canard arrangement. Thus, the main region of interest is canard arrangement and its aerodynamic effects. The missile body was designed at the aft section to give structural support to the canard arrangement and thus its aerodynamic effects on it are not taken into consideration.

Design 1: Spherical canard arrangement.

Design 2: Notched canard arrangement.

A 2D model of the missile with a nose cone and canard arrangement and half body of the missile was designed and analysed in supersonic flow conditions. A 2D model was designed because the missile/rocket body and canard arrangements possess the symmetric shape.

Design 1: The spherical canard model was of totally1 unit length (because GAMBIT does not have any units but FLUENT has), the Canard hinge point starts at 0.5 units and ends at 0.625 units. The nose cavity is of arc length of 0.039 units. The spherical canard is of arc length of 0.266 units. The farfield has got a vertical length of 3.25 units and horizontal length of units of 3.

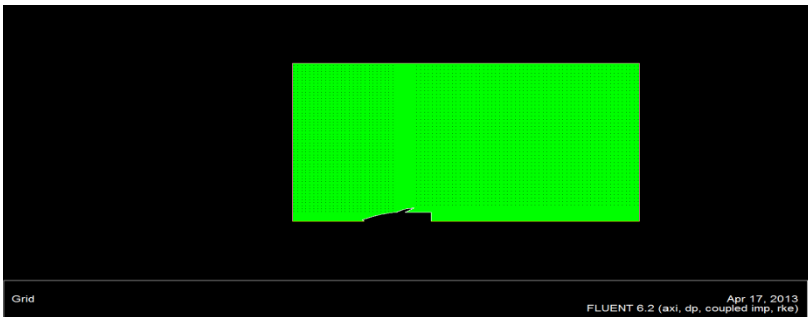

Figure: 4.1. Grid view of the missile model with spherical canard

Design 2: The notched canard model is of total unit length of 1 .The nose curvature is of arc length of 0.039 units and canard arc length is of 0.039 units.Similarly,thefarfield conditions are of 3.25 and 3 units along vertical and horizontal axis respectively,

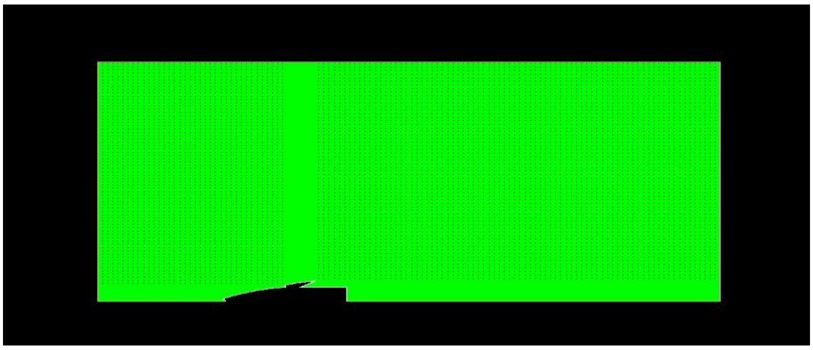

Figure: 4.2. Grid view of the missile with the notched canard arrangement

VI. INPUTS GIVEN

In this section the various inputs given in the software were analysed;

A. Mesh consideration.

For this 2D model quadrilateral meshes were used. At the edges mesh interval size of 0.01 was used and in region of interest (i.e. around the model) a fine mesh count of 100 was used. Thus, a region of fine mesh surrounded by a region of coarse mesh was created. Meshes were used to capture the air flow/shocks near to the model. This study uses the shock capturing technique FVM study [8].Swapping forward method [9] was used to create the mesh domains. This quadrilateral cell arrangement supports to capture the shock and it can reduce the skewness factor.

B. Boundary consideration.

The boundary conditions used in the design models of the following;

S.no	**Boundary conditions**	**Edges taken**
1.	Pressure farfield	All except wall ,symmetry
2.	Wall	The model.
3.	Symmetry	The base of the model& base line of the farfield.

TABLE: IV.1.BOUNDARY CONDITIONS

C. *Initial Conditions.*

The mesh files were saved after giving the boundary conditions and then exported as 2 D mesh. The mesh case files were studied using ANSYS FLUENT [10], a commercial FVM coded software. The initial conditions were same for both the models.

A **density based solver** was chosen for the study. This is because density based solver possess inbuilt criteria of solving high heat and viscous effect problems. **Energy equation** was taken into consideration (because this supersonic study involves high heat and viscous effects).In the viscous models, aRealizable**K-E** two equation model was taken into consideration-E model was used in the case of supersonic and hypersonic cases. The two equation model has got the kinetic energy and heat dissipation rate as two solvable equations. Thus, the problem was solved under **Ideal gas** conditions. In the ideal gas condition dialogue box put the following values;

Cp value 0f 1.006 J/kg-K,with a viscosity of 1.789*10^-05 Kg/m-s and with a thermal conductivity value of
0.0204 W/m-K.In the boundary conditions set farfield as **Pressure farfield**with **Mach number of 3** and gauge pressure of **18800 Pa (these values were found from the ISA tables).**Set wall conditions to the whole missile body with canards.

In the initialization dialogue initialize the **pressure farfield** with **a axial velocity of 1022 m/s**(Mach number 3) and **with gauge pressure value of 18800 Pa**.Isothermal**static temperature was kept at 300K**.The **convergence criteria was set at 10^6 and courant number was kept at 0.1**(this determines stability of the solution).Solve the solution with highest order of convergence for Navier-stokes solution (i.e. **Second order discretization**).Initially iterate the solution for upto 1000 iterations for seeing the degree of convergence.Then,shift the value of iteration to about10,000 for complete convergence.

Short summary of above details;

1. Density based solver.
2 Energy equation.
3 Realizable K E flow model.
4 Ideal gas flow.

D. *Equations used.*

The model was solved with K E viscous flow model.The viscous Navier stokes equation was used along with the equation of Continuity; Energy and Momentum equations were solved. The model comes under conservative form of viscous flow model as model was fixed within the flowing velocity field [Source: Introduction to CFD by J.D.Anderson].These equations were solved for upto 10,000 iterations to meet the convergence criteria;

1. Continuity Equation

$$\frac{d\rho}{dt} + \nabla.(\rho V) = 0 \qquad (\mathbf{5.1})$$

2. Momentum Equation

X axis: $\partial\left(\frac{\rho U}{\partial t}\right) + \nabla.(\rho u V) = -\frac{\partial P}{\partial x} + \frac{\partial \tau \mathrm{xx}}{\partial \mathrm{x}} + \frac{\partial \tau \mathrm{xy}}{\partial \mathrm{y}} + \frac{\partial \boldsymbol{\tau} \mathrm{xz}}{\boldsymbol{\partial} \mathbf{z}}$ **(5.2)**

Y axis: $\partial\left(\frac{\rho V}{\partial t}\right) + \nabla.(\rho v V) = -\frac{\partial P}{\partial y} + \frac{\partial \tau \mathrm{xy}}{\partial \mathrm{x}} + \frac{\partial \tau \mathrm{yy}}{\partial \mathrm{y}} + \frac{\partial \boldsymbol{\tau} \mathrm{yz}}{\boldsymbol{\partial} \mathbf{z}}$ **(5.3)**

Z axis: $\partial\left(\frac{\rho W}{\partial t}\right) + \nabla.(\rho w V) = -\frac{\partial P}{\partial z} + \frac{\partial \tau \mathrm{xz}}{\partial \mathrm{x}} + \frac{\partial \tau \mathrm{zy}}{\partial \mathrm{y}} + \frac{\partial \boldsymbol{\tau} \mathrm{zz}}{\boldsymbol{\partial} \mathbf{z}}$**(5.4)**

3. Energy Equation.

$$\begin{aligned}
&\partial[\rho(e + V^2)] + \nabla[\rho(e + V^2)V] \\
&\quad = \rho q + \left(\frac{\partial}{\partial x}\right)\left(\frac{K\partial T}{\partial x}\right) + \left(\frac{\partial}{\partial y}\right)\left(\frac{K\partial T}{\partial y}\right) + \left(\frac{\partial}{\partial Z}\right)\left(\frac{K\partial T}{\partial Z}\right) - \partial\left(\frac{UP}{\partial x}\right) - \partial\left(\frac{VP}{\partial y}\right) - \partial\left(\frac{WP}{\partial Z}\right) \\
&\quad + \left(\frac{\partial}{\partial x}\right)(U\boldsymbol{\tau xx}) + \left(\frac{\boldsymbol{\partial}}{\boldsymbol{\partial y}}\right)(\boldsymbol{U\tau xy}) + \left(\frac{\boldsymbol{\partial}}{\boldsymbol{\partial z}}\right)(\boldsymbol{U\tau xz}) + \left(\frac{\boldsymbol{\partial}}{\boldsymbol{\partial z}}\right)(\boldsymbol{V\tau xz}) + \left(\frac{\boldsymbol{\partial}}{\boldsymbol{\partial x}}\right)(\boldsymbol{V\tau xy}) \\
&\quad + \left(\frac{\boldsymbol{\partial}}{\boldsymbol{\partial y}}\right)(\boldsymbol{V\tau yy}) + \left(\frac{\boldsymbol{\partial}}{\boldsymbol{\partial z}}\right)(\boldsymbol{V\tau yz}) + \left(\frac{\boldsymbol{\partial}}{\boldsymbol{\partial x}}\right)(\boldsymbol{V\tau yx}) + \left(\frac{\boldsymbol{\partial}}{\boldsymbol{\partial y}}\right)(\boldsymbol{V\tau yy}) + \left(\frac{\boldsymbol{\partial}}{\boldsymbol{\partial z}}\right)(\boldsymbol{W\tau xz}) \\
&\quad + \left(\frac{\boldsymbol{\partial}}{\boldsymbol{\partial y}}\right)(\boldsymbol{W\tau yz}) + \left(\frac{\boldsymbol{\partial}}{\boldsymbol{\partial z}}\right)(\boldsymbol{W\tau zz}) + \boldsymbol{\rho f V}. \quad (\mathbf{5.5})
\end{aligned}$$

4. Standard K-E model.
Standard K-E model includes the combination of both the kinetic energy transfer and energy dissipation rate. Equation (5.6) constitutes the kinetic energy equation, whereas equation (5.7) constitutes the heat dissipation rate equations.

$$\frac{\partial(\rho k)}{\partial t} + div(\rho k U) = div\left[\frac{\square}{\sigma} gradk\right] + 2\square S_{ij} S_{ij} - \rho\dot{\varepsilon} \quad \mathbf{(5.6)}$$

$$\frac{\partial(\rho\dot{\varepsilon})}{\partial T} + div(\rho\dot{\varepsilon} U) = div\left[\frac{\square}{\dot{\varepsilon}} grad\dot{\varepsilon}\right] + C1_{\dot{\varepsilon}}\frac{\dot{\varepsilon}}{k} 2\square S_{ij} S_{ij} - C_{2\dot{\varepsilon}}\rho\dot{\varepsilon}^2/k \qquad \mathbf{(5.7)}$$

These equations were solved for upto 10,000 iterations to meet the convergence criteria.

VI.RESULTS (i.e. Physical Interpretation)

In this section various obtained contour plots of the results were shown and the aerodynamic variations were discussed,

1. Pressure contours.
2. Velocity contours
3. Temperature contours.
4. XY plots.

(A).PRESSURE CONTOURS.

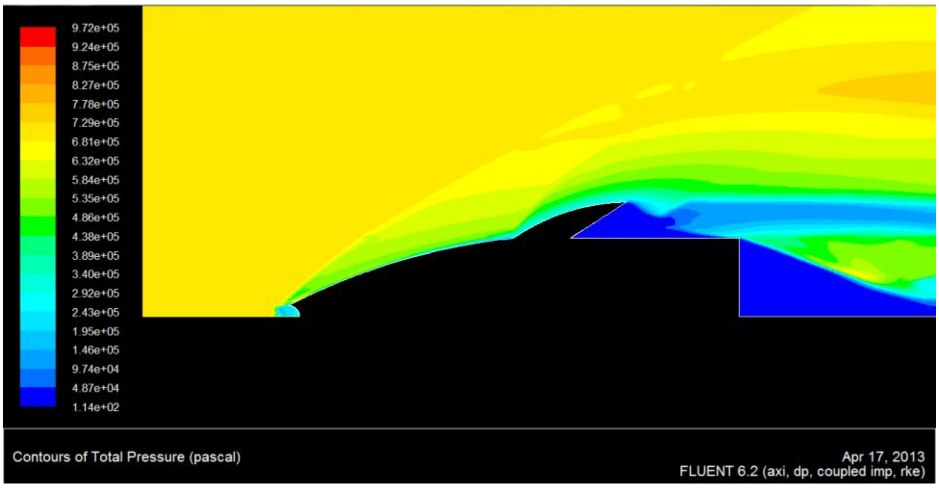

Figure: 6.1. Pressure Distribution over the missile with spherical canards

Figure (6.1) shows the total pressure distribution over the supersonic cruise missile with spherical canard at Mach speed of 3.The missile was computationally tested at tropospheric altitude of 12 Km (i.e. about 40,000 ft.) above mean sea level. From the pressure contours it was found that in our region of interest (the canard region) experiences high pressure region. This is due to formation of reattached bow shock. Behind the canard and body a region of low pressure exists. This is due to formation of vortex (wake formations) in that region.

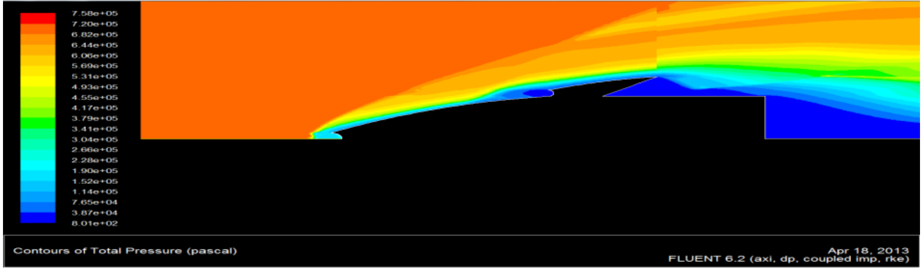

Figure: 6.2. Pressure Distribution over the missile with notched canards.

Figure (6.2) shows the pressure distribution over the missile body with notched canard arrangement. In our region of interest the pressure distribution is less when compared to the spherical canard model. This occurs due to the formation of region of circulation (wakes) at the front and at notched canard front region.

(B).VELOCITY CONTOURS.

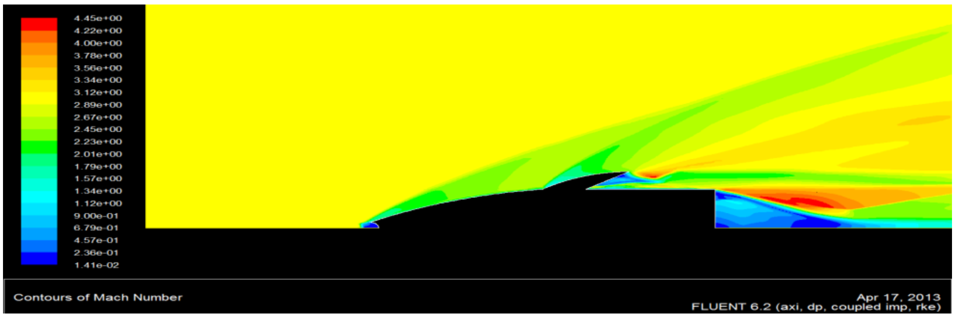

Figure: 6.3. Velocity Distribution over the missile with spherical canard arrangement.

The velocity contours of figure 6.3. explains that a region of bow shock had occurred ahead of the body due to high turbulent and pressure actions. Near to the spherical canard region one can see high Mach number flows.

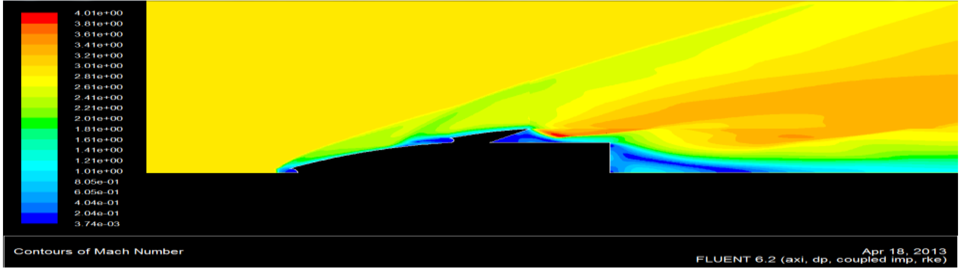

Figure: 6.4. Velocity Distribution over the missile with notched canard arrangement.

From the figure 6.4.the velocity distribution over the notched canard arrangement was clearly visible. A low Mach number flow was witnessed near to the region of nose and our area of concern; the canard region. This occurs due to reduce of the pressure and wave drag in that region.

(C).TEMPERATURE DISTRIBUTION.

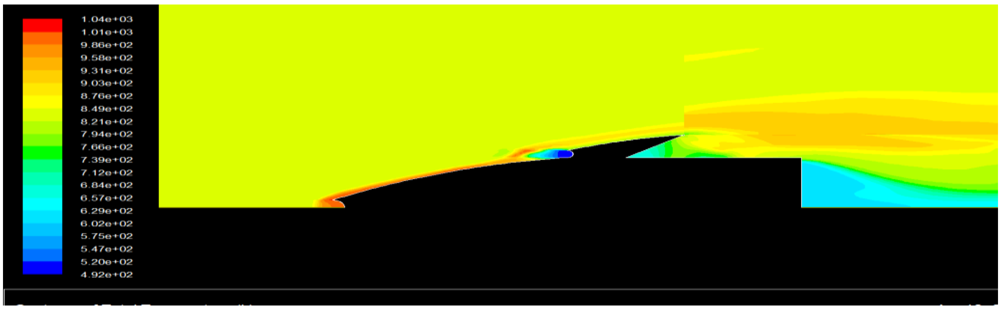

Figure: 6.5. Temperature Distribution over the missile model with notched canard arrangement.

Now, we have come to our area of research section. As I have already mentioned that the total temperature distribution near to the notched canard region would be very less. The statement was proved from the figure 6.5.shown above. Thus, only in that notched region aerodynamic heating was less when compared to other portions of the body. The reason could be high vorticity.Thus; this model prevents canards from high aerothermodynamicheating. This region is well suited for placing sensors and other heat sensitive materials.

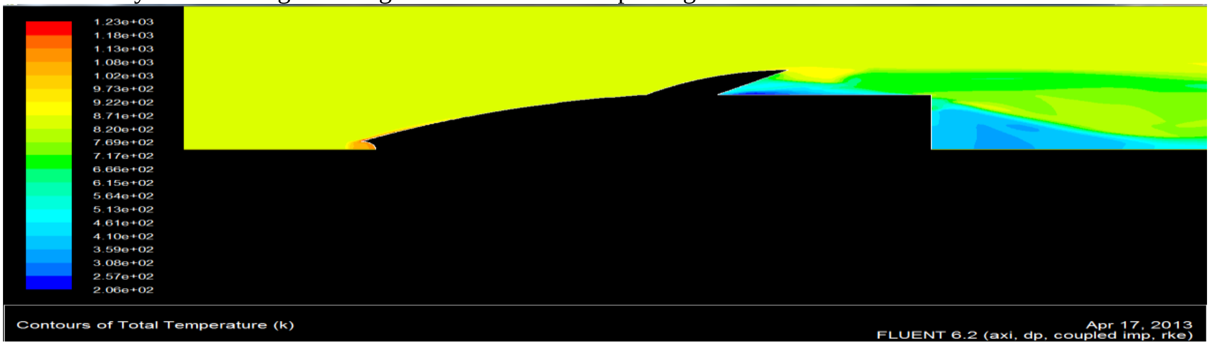

Figure: 6.6. TemperatureDistribution over the missile with spherical canard arrangement.

The results obtained from figure.6.6. was found to be vice-versa to the notched region results. A high temperature region was present near to the canard region, which would result in high heating in that region, which would at last causes some dynamic instability problem to the missile's rotatory motion.

(D).XY PLOTS.

Missile with Spherical Canards Missile with Notched Canards.

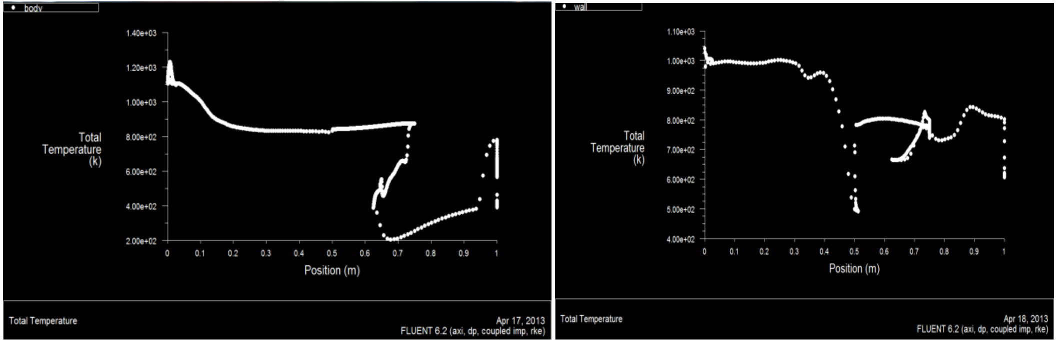

Figure: 6.7.XY Temperature plots of themodels.

The canard arrangement starts at a length of 0.5 m from the nose point. By comparing both the plots at 0.5m high temperature is found in the spherical canard and region of low temperature in notched canard arrangement.

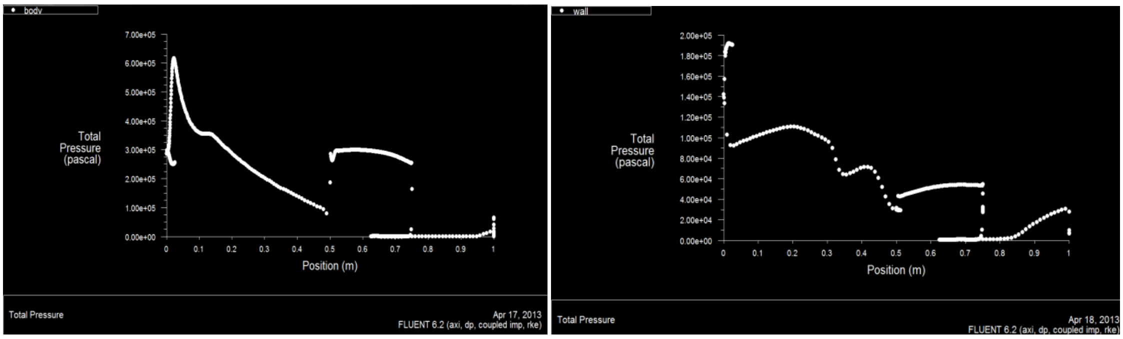

Figure: 6.8.XY Pressure plots of the models.

At the canard arrangement region of 0.5m a region of high pressure was found in spherical model when compared to the notched canard model**.**

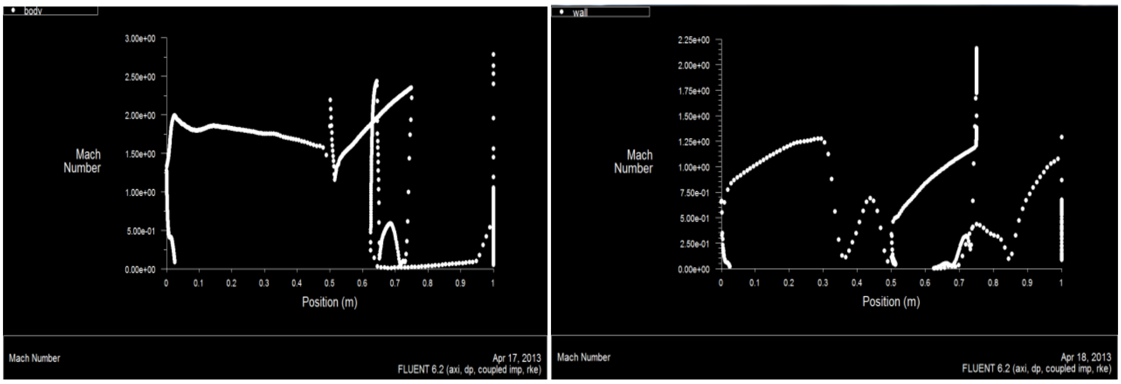

Figure: 6.9.XYMach number plot over the models.

Mach number plot shows that there occurs fluctuating flow of air at all points. Thus, when comparing the canard arrangement area of both the models. A region of high Mach number was found in the spherical case when compared to the notched case.

(E).VECTOR PLOTS.

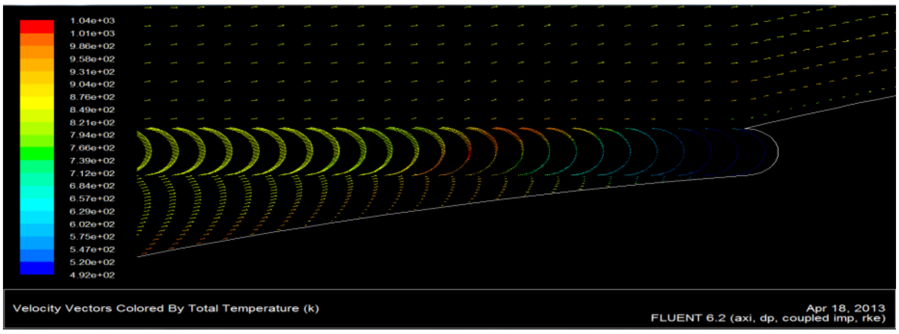

Figure: 6.10.Vectorplot near to the notched region of the missile

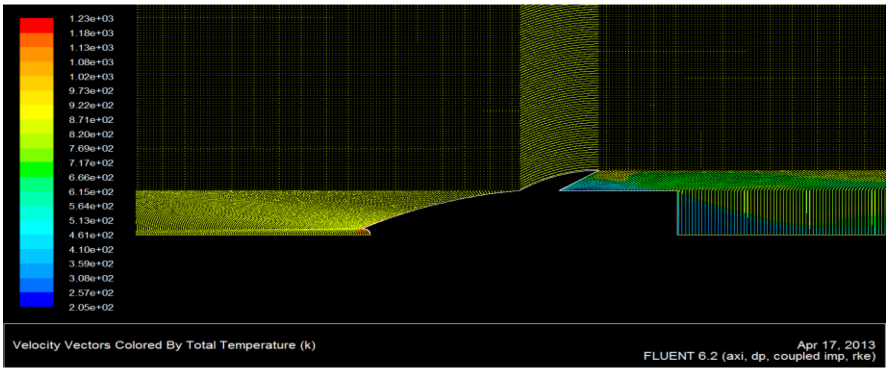

Figure: 6.11. Vectorplot of the spherical canard model.

By considering both the models it was found that there occurs a region of circulation near to the cavity region of the notched model. Such circulations were not found in the spherical model. Thus, circulation is the main causes for temperature reduce in the cavity region.

VII. CONCLUSION

Mach number in the range of 1 to 3 constitutes the region of supersonic flows. In the supersonic region when a body is placed it surely experiences a shock. It can be either bow shock or normal shock that is based on the shape of the body. In this region high viscous effects are prominent. Mach number values before and after shock changes a lot. [7].

In supersonic flow stream shock moves mostly in downstream angle. Canards offer rotational stability to the model. But, canards are region where gravitational sensors are placed. Therefore, the, the canard region should experience a region of low surface temperature distribution. Various models were studied and the notched cavity model was found very effective. This arrangement offers low surface heating in that hinge point region of the canard. It also offers less weight as some portion of it canards was removed. It also offers good rotational stability. From the results by comparing the models it was found that the spherical canard arrangement has got a surface temperature of 870K at the canard hinge point. But, in the proposed model the canard model possess a surface temperature effect of 492K.Similarly, the pressure distribution in the spherical canard region is of 3.42 *10^5 Pa and Similarly, in the region of notched canard arrangement the pressure distribution was found to be 8.01*10^2 Pa. Thus, the proposed model was found very effective in temperature resistance when compared to the present models of the canards.

APPENDIX.

This appendix consists of a simple FORTRAN 90 code of solving pressure equations for rocket trajectory analysis**.**

```
programtroposphericcalculations
!to calculate the pressure below and above the troposphere
real p0,h,t0,p
real p11,g,h11,r,t11
print*,'enter the value of initial pressure p0'
read*,p0
print*,'enter the value of initial temperature t0'
read*,t0
```

```
print*,'enter the value of specified height h'
read*,h
h11=11 !troposphere starts from this height
p11=226.32 !pressure above the tropospheric layer
t11=216.52 !temperature above the tropospheric layer
r=287 !gas constant
call below(p0,h,t0,p)
call above(p1,p11,g,h,h11,r,t11)

end program tropospericcalculations
subroutinebelow(p0,h,t0,p)
p=p0(1-0.0065*h/t0)**(52561)
print*,'the value of pressure below the troposphere is::',p
end subroutine
subroutine above(p1,p11,g,h,h11,r,t11)
p1=p11*exp(-(g)*(h-h11)/(r*t11))
print*,'the value of pressure above the troposphere is::',p1
end subroutine
```

ACKNOWLEDGEMENT

We would like to express our deep acknowledgement to Dr.UgurGuven, HOD, Dept. of CFD, UPES-Dehradun for helping students in the field of research and development. We would also like to express our thankfulness to Mr.KarthikSundarraj, Mr.SourabhPramodBhatof Dept.of.Aerospace for providing technical supports.

.

REFERENCES

[1]. Mustafa Cavcar, AnadoluUniversity, Turkey. (2009). the International Standard Atmosphere. Pages 12.

[2]. Rajesh Yadav, UgurGuven, GurunadhVelidi. (2012). Aerothermodynamics of Generic Reentry vehicle with a series of Aerospikes at nose. International Astronautical Congress. , pg. 1-9

[3]. K. Sridhar, T. Vijayalakshmi, I. Balaguru, S. Senthilkumar. (2012). Computational fluid dynamic analysis of Missile with Grid fins. ActaTechnicaCorviniensis. Volume 4, Pg.93-96

[4]. J Sreenivasulu, Dr. Patil M M, E Sivaramakrishnan. (2010). Aerodynamic Analysis of a Rocket Configuration with Grid Fin. International Conference on Fluid Mechanics and Fluid Power. , pg.1-5.

[5]. Jackson E. Fowler et al. (2013). Transonicbuckets for Axial flow turbines. Pages4.

[6]. Grid fins. Available: http://en.wikipedia.org/wiki/Grid_fin. Last accessed 18th April 2013.

[7]. B.Kaleeswaran, S.Ranjith Kumar, Jeniwer Bimro.N. (2013). An Aerodynamic Optimization of Supersonic Flow Over The Nose Section of Missiles. International Journal of Engineering Research & Technology. Volume2, Issue 4, pg.453-462.

[8]. H.Versteeg, W.Malalasekra (2009). An Introduction to Computational Fluid Dynamics: The Finite Volume Method. 2nd edition. New Delhi: Pearson Education Ltd.

[9]. J.D.Anderson (1995). *Computational Fluid Dynamics*. 3rd ed. New York: McGraw-Hill Education. 587.

[10]. ANSYS FLUENT 12.0.